

Synthesis and Physical Properties of a "Double-Cable" Polymer for Photovoltaic Applications

Ali Mohammed Alsalmeh^{1,*}, Abdulaziz Ali B. Alghamdi¹, Ateyyah M. Al-Baradi² and Ahmed Iraqi³

¹ Department of Chemistry, College of Science, King Saud University, PO Box 2455, Riyadh 11451, Saudi Arabia.

² Department of Physics, Taif University, Taif 888, Saudi Arabia.

³ Department of Chemistry, University of Sheffield, Sheffield S3 7HF, UK

* E-mail: aalsalme@ksu.edu.sa

Received: 10 February 2013 / Accepted: 15 March 2013 / Published: 1 April 2013

A novel "double cable" polymer was developed. Which are generally composed of a carbazole-bithiophene backbone functionalised with perylene tetracarboxylic diimide (PDI) units as electron acceptors, to avoid phase separation problems between donors and acceptors. The study on the physical properties of the polymer and the interaction of the perylene diimide electron accepting substituents with the polymer backbones in this class of "double cable" polymers is presented.

Keywords: Conjugated polymers; double cable polymer; solar cells.

1. INTRODUCTION

One of the main problems of problems of the bulk heterojunction solar cells is the phase separation between the donor and acceptor within active layer due to limited miscibility. This problem influences negatively the photoinduced charge separation and the photoinduced charge transfer between donor and acceptor and consequently reduced the efficiency of the solar cell [1,2]. A convenient way to overcome this problem and insure a large interfacial area between donor and acceptor is to control the morphology of active layer by preparing "double cable" polymers where the electron acceptor moieties are attached directly to the conjugated polymer chain by covalent grafting. This arrangement guarantees a more homogeneous distribution of donor and acceptor domains compared to bulk hetero junction structure, and the generated electrons (by photoinduced electron transfer) is transported by hopping between the acceptor moieties [3,4,5].

The photoinduced charge transfer from the donor chain to the pendant acceptor can be studied by photoinduced absorption spectroscopy and by light induced ESR spectroscopy [6].

The double cable polymers have to meet the following requirements:

- 1) The ground-state electronic properties are independent of the donor backbone and the acceptor moieties and there is no interaction between them.
- 2) Photoinduced charge transfer from donor to acceptor leading to long lived charged states [7].

In 2001 Ramos et al. reported the first use of double cable polymers in organic solar cell by using a PPV derivative, with QE of 6% [8]. In the same year Zang et al. reported solar cells based on polythiophene double cable polymers with a PCE of 0.6% [9].

Perylenediimide (PDI) has received a great interest in researches where PDI derivatives have been developed into one of the best acceptors (n-type), and they have been widely used in different applications such as thin-film transistors, solar cells, liquid crystals and electron transporting components in organic light-emitting diodes due to their high thermal, chemical, and photochemical stability. Also Perylenediimides represent high thermostable n-type semiconductors with good transport property and high electron affinity [10].

In addition, they are able to form self-organised architectures due to their inherent π -system interactions that increase exciton diffusion length and improve mobility of charge carriers which in turn improve the performance of devices [11]. Moreover, perylenediimide derivatives have been covalently linked as side chains to conjugated polymers such as poly(methylmethacrylate) and poly(isocyanide). These polymers show efficient energy transfer to the pendant groups which observed in the photoluminescence spectrum [13].

2. EXPERIMENTAL SECTION

2.1 Materials

All chemicals and were purchased from the commercial suppliers and used as received unless otherwise stated. All solvent used for the reaction were dried except t-BuOH, N,N-dimethylacetamid and acetone. The reactions for preparing monomers were carried out under Nitrogen atmosphere and the reaction for preparing polymer was carried under Argon atmosphere.

2.2 Measurements

NMR Spectra were recorded on Bruker 250 MHz, AMX400 400 MHz or DRX500 500 MHz NMR spectrometers at 22 °C in chloroform- d_1 , acetone- d_6 and 1,1,2,2-tetrachloroethane- d_2 solution with TMS as the internal standard. IR absorption spectra were recorded on the Nicolet Model 205 FT-IR Spectrometer using a Diamond ATR attachment for solid samples analysis. Mass spectra were recorded on Perkin Elmer Turbomass Mass Spectrometer Equipped with Perkin Elmer PE-5MS Capillary Column for GCMS. MS was obtained *via* chemical ionization (CI) or electron impact (EI)

methods. MALDI-TOF spectra were recorded on a Bruker Reflex III in reflection positive ion mode with a DCTB matrix.

Elemental analysis was carried out by the Perkin Elmer 2400 CHN Elemental Analyzer for CHN analysis and by the Schöniger oxygen flask combustion method for anion analysis. The weights of the samples submitted for analysis were approx. 5 mg for CHN analysis and approx. 5 mg for each anion analysis. Melting points were measured using a Linkam HF591 heating stage in conjunction with a TC92 controller.

GPC curves were recorded on an equipment consisting of a Hewlett Packard Model 1090 HPLC, a Hewlett Packard Model 1037 Differential Refractive Detector, two Polymer Labs PLgel 5 μ Mixed C (300 mm x 7.5 mm) columns and a guard (50 mm x 7.5 mm) using CHCl₃ (HPLC grade) as the eluent at a rate of 1 cm³ min⁻¹. Polymer samples were made up as solutions in chloroform (2.5 mg cm⁻³) spiked with toluene as a reference. The GPC curves were obtained by the RI-detection method, which was calibrated with a series of narrow polystyrene standards (Polymer Laboratories).

UV-visible absorption spectra were measured by Hitachi U-2010 Double Beam UV / Visible Spectrophotometer. The absorbance of polymers was measured in solution of toluene (spectrophotometric grade) and THF (spectrophotometric grade) at ambient temperature using rectangular quartz cuvettes (light path length = 10 mm) purchased from Sigma-Aldrich. Samples of pristine polymer thin films for UV-visible absorption spectra measurements were prepared by dip coating quartz plates into 1 mg cm⁻³ polymer solutions in chloroform (HPLC grade) and the measurements were carried out at ambient temperature.

Photoluminescence spectra were obtained using the Hitachi F-4500 Fluorescence Spectrophotometer equipped with Hamamatsu Photonics R928F Photomultiplier Tube (PMT). PL solution measurements were carried out using a Quartz Fluorescence Cuvette (light path length = 10 mm) purchased from Sigma-Aldrich. All measurements were carried out in dilute solutions of toluene (spectrophotometric grade) and THF (spectrophotometric grade) at 25 °C temperature in the air. The UV/vis absorbance of the samples was kept below 0.1 in order to obtain PL spectra free from inner-filter effects. Samples of polymer and monomer thin films for PL spectra measurements were prepared by dip coating quartz plates into 0.1 mg cm⁻¹ polymer solutions in chloroform (HPLC grade, which were then dried in the air.

Cyclic voltammograms were recorded with a Princeton Applied Research model 263A Potentiostat/Galvanostat. Measurements were carried out under argon at 25 \pm 2 °C. Tetrabutylammonium tetrafluoroborate (TBABF₄, 10 cm³) solution in acetonitrile (0.1 mol dm⁻³) was used as the electrolyte solution. A three-electrode system was used consisting of an Ag/Ag⁺ reference electrode (silver wire in 0.01 mol dm⁻³ silver nitrate solutions in the electrolyte solution), a platinum working electrode (2-mm diameter smooth platinum wire), and a platinum counter electrode (platinum wire). Polymer thin films were prepared by drop casting 1.0 mm³ of polymer solutions in dichloromethane (HPLC grade) (1 mg cm⁻³) onto the working electrode then dried in air.

DSC curves were recorded on Perkin Elmer Pyris 1 Differential Scanning Calorimeter equipped with Perkin Elmer CCA7 Sub ambient Accessory at the scan rate of 10°C/minute under inert nitrogen atmosphere. Aluminum pans were used as sample pans. An empty aluminum pan was used as

the reference. TGA curves were obtained by Perkin Elmer TGA-7 Thermogravimetric Analyser at a scan rate of 10 °C/minute under inert nitrogen atmosphere.

2.3 Synthesis

All reactions were carried out under inert nitrogen atmosphere.

Undecylododecylamine (1)

Undecylododecylamine was prepared according to a modified procedure by Che *et al* [16]. A solution of sodium cyanoborohydride (3.2 g; 50.9 mmol) and ammonium acetate (40 g; 518.9 mmol) in dry methanol (200 ml) was transferred into a solution of 12-tricosanone (17.8 g; 52 mmol) in dry THF (450 ml). This mixture was stirred for 55 hours at room temperature and then concentrated HCl (8 ml) was added. The mixture was then concentrated by rotary evaporator before THF (80 ml) was added followed by the addition of H₂O (1000 ml). The pH of the mixture was adjusted to approx. pH 10 with KOH flakes and the obtained dispersion was extracted with CHCl₃ (3 x 300 ml). The organic phase was concentrated to obtain a pale yellow oil which crystallized to a white solid (17.7 g, 99.1% yield). ¹H NMR (CDCl₃) δ_H/ ppm: 2.71 (m, 1H); 1.47-1.18 (m, 40H); 0.89 (t, 6H). ¹³C NMR (CDCl₃) δ_C/ ppm: 51.59, 36.01, 33.65, 31.91, 29.85, 29.64, 29.35, 25.82, 25.63, 22.67, 14.07. Elemental analysis (%) calculated for C₂₃H₄₉N: C, 81.33; H, 14.54; N, 4.12. Found: C, 80.79; H, 14.86; N, 3.43. Mass (EI+); (m/z): 336, 338, 339 (M+•); (calculated for C₂₃H₄₉N: 339.64).

N,N'-di(1-Undecylododecyl)-perylene-3,4:9,10-tetracarboxylic diimide (2)

N,N'-di(1-Undecylododecyl)-perylene-3,4:9,10-tetracarboxylic diimide was prepared according to a modified procedure by Balakrishnan *et al* [12]. A mixture of 1-Undecylododecylamine (16.68 g, 49.11 mmol), perylene-3,4,9,10-tetracarboxylic dianhydride (7.65 g, 19.49 mmol) and imidazole (57.5 g, 844.56 mmol) was heated at 140° C for 4 hours. Then the mixture cooled down to room temperature and the obtained red solid was dispersed in 550 ml of ethanol followed by addition of 1700 mL 2 M HCl and stirred overnight. The obtained red solid was filtered and washed with distilled water until the pH of washing was neutral and dried under vacuum for 6 hours (16.75g, 82.96% yield). The product gave a single spot on TLC (100% chloroform) (R_f = 0.89). ¹H NMR (CDCl₃) δ_H/ ppm: 8.64 (m, 8H); 5.20 (m, 2H); 2.25 (m, 4H); 1.89 (m, 4H); 1.19 (m, 72H); 0.86 (t, 12H). ¹³C-NMR (CDCl₃) δ_C/ ppm: 164.62, 163.55, 134.46, 131.86, 131.08, 129.57, 126.41, 123.91, 123.19, 122.96, 54.75, 32.35, 31.88, 31.75, 30.53, 29.59, 29.56, 29.52, 29.30, 28.64, 26.95, 22.64, 14.07. FT-IR (ATR): (ν̄/cm⁻¹): 2918.3, 2849.2, 1692.0, 1648.5, 1592.4, 1577.0, 1466.1, 1404.8, 1336.9, 1251.8, 1175.3, 812.2, 749.7, 721.6. Elemental analysis (%) calculated for C₇₀H₁₀₂N₂O₄: C, 81.19; H, 9.93; N, 2.71; O, 6.18. Found: C, 77.65; H, 9.06; N, 2.54. MALDI-TOF MS (monoisotopic mass = 1035.6); m/z = 1035 [M + H⁺].

N-(1-undecylododecyl)-3,4,9,10-perylenetetracarboxylic acid 3,4-anhydride-9,10-imide (3)

N-(1-undecylododecyl)-3,4,9,10-perylenetetracarboxylic acid 3,4-anhydride-9,10-imide was prepared according to a modified procedure by Chen *et al* [16]. A mixture of N,N'-di(1-Undecylododecyl)-perylene-3,4:9,10-tetracarboxylic diimide (11 g, 10.62 mmol) and ground KOH (1.71 g, 30.59 mmol) in 200 ml of t-BuOH was heated to reflux under N₂ for 30 min. A further portion of KOH (0.174 g, 3.11 mmol) was added and the mixture was held at reflux for one hour. The mixture was then cooled down to 0° C. A mixture of glacial acetic acid and 2M HCl (520 ml, 1:4 v/v) was

added with stirring. The mixture was stirred overnight. The obtained red precipitate was filtered off and washed with large amount of H₂O and 10 % w/v NaCl. The crude product was then purified via gel silica column chromatography, eluting with 99:1 chloroform/AcOH. (5.35 g, 70.6% yield). The product gave a single spot on TLC (99:1 CHCl₃/AcOH) (R_f = 0.32). ¹H NMR (CDCl₃) δ_H/ ppm: 8.67 (m, 8H); 5.19 (m, 1H); 2.29 (m, 2H); 1.89 (m, 2H); 1.20 (m, 36H); 0.84 (t, 6H). ¹³C-NMR (CDCl₃) δ_C/ ppm: 164.31, 163.21, 159.80, 136.23, 133.41, 131.88, 131.68, 131.12, 129.38, 126.61, 126.37, 124.71, 123.97, 123.84, 123.02, 118.85, 54.90, 32.29, 31.86, 29.56, 29.55, 29.50, 29.22, 26.94, 22.64, 14.08. Elemental analysis (%) calculated for C₄₇H₅₅NO₅: C, 79.07; H, 7.76; N, 1.96; O, 6.18. Found: C, 79.34; H, 8.18; N, 2.01.

4.3.4 N-(1-undecyldodecyl)-N'-(6-hydroxyhexyl)perylene-3,4,9,10-tetracarboxylic diimide (4)

N-(1-undecyldodecyl)-N'-(6-hydroxyhexyl)perylene-3,4,9,10-tetracarboxylic diimide was prepared according to a modified procedure by Jancy *et al* [17]. A mixture of 6-aminohexanol (0.479 g, 4.087 mmol) and zinc acetate (0.01 g, 0.054 mmol) in N,N'-dimethylacetamide (DMAC) (39 ml) was heated to 110° C, then N-(1-undecyldodecyl)-3,4,9,10-perylenetetracarboxylic acid 3,4-anhydride-9,10-imide (1.94 g, 2.717 mmol) was added. The reaction mixture was stirred for 3 h at 110° C then the temperature was increased to 160° C for 15 h. The excess solvent was removed via distillation under vacuum and the obtained slurry was dissolved in chloroform and washed with H₂O (4 x 500 ml). The organic layer was concentrated and the solid product was purified via gel silica column chromatography, eluting with 99:1 chloroform/AcOH to obtain red solid (2.2 g, 99.4% yield). The product gave a single spot on TLC (99:1 CHCl₃/AcOH) (R_f = 0.33). ¹H NMR (CDCl₃) δ_H/ ppm: 8.635 (m, 8H); 7.814 (d, 2H, J = 8.31 Hz); 7.373 (d, 2H, J = 8.07 Hz); 5.204 (m, 1H); 4.172 (t, 2H, J = 7.38 Hz); 4.053 (t, 2H, J = 6.48 Hz); 2.472 (s, 3H); 2.266 (m, 2H); 1.895 (m, 2H); 1.718 (m, 4H); 1.421 (m, 4H); 1.212 (m, 36H); 0.854 (t, 6H, J = 6.85 Hz).

N-(1-Undecyldodecyl)-N'-(6-hexyl-p-toluenesulfonate)perylene-3,4,9,10-tetracarboxylic diimide (5)

N-(1-Undecyldodecyl)-N'-(6-hexyl-p-toluenesulfonate)perylene-3,4,9,10-tetra carboxylic diimide was prepared according to a modified procedure by Yoshida *et al* [16]. A solution of p-toluenesulfonyl chloride (2.14 g, 11.22 mmol) in CH₂Cl₂ (14 ml) was cooled down to 0 - 5° C and added to a mixture of trimethylamine hydrochloride (0.2764 g, 2.89 mmol), N-(1-undecyldodecyl)-N'-(6-hydroxyhexyl)perylene-3,4,9,10-tetracarboxylic diimide (2.11 g, 2.59 mmol) and Et₃N (2.28 ml) in CH₂Cl₂ (14 ml) at 0 - 5° C. The reaction mixture was stirred at 0 - 5° C, then water was added. The reaction mixture was extracted with CH₂Cl₂ and the collected organic layer were washed with water and then concentrated. The solid product was purified via gel silica column chromatography, eluting with 99:1 chloroform/AcOH to obtain red solid (2.41 g, 96% yield). The product gave a single spot on TLC (99:1 CHCl₃/AcOH) (R_f = 0.44). ¹H NMR (CDCl₃) δ_H/ ppm: 8.548 (m, 8H); 7.807 (d, 2H, J = 8.18 Hz); 7.366 (d, 2H, J = 7.85 Hz); 5.196 (m, 1H); 4.151 (t, 2H, J = 14.775 Hz); 4.049 (t, 2H, J = 12.9 Hz); 2.465 (s, 3H); 2.266 (m, 2H); 1.886 (m, 2H); 1.682 (m, 4H); 1.312 (m, 4H); 1.207 (m, 36H); 0.845 (t, 6H, J = 6.925 Hz). ¹³C NMR: (CDCl₃) δ_C/ppm: 164.52, 163.40, 163.19, 144.63, 134.49, 134.10, 133.21, 131.71, 131.21, 130.94, 129.81, 129.42, 129.18, 128.87, 126.25, 126.14, 124.02, 123.27, 123.21, 122.96, 122.84, 70.47, 54.82, 40.31, 32.34, 31.88, 29.62, 29.57, 29.55, 29.31, 28.73, 27.82, 26.95, 26.41, 25.12, 22.65, 21.64, 14.06. Elemental Analysis (%) Calculated for C₆₀H₇₄N₂O₇S:

C, 74.50%; H, 7.71%; N, 2.90%; S, 3.31%. Found: C, 74.20%; H, 7.79%; N, 2.82%; S, 3.55%. MALDI-TOF MS (monoisotopic mass = 967.3); $m/z = 966.4 [M + H^+]$.

N-9'-[*N*-(1-undecyldodecyl)-*N*'-(6-hexyl)perylene-3,4,9,10-tetracarboxylic diimide]-2,7-dibromocarbazole (6)

N-9'-[*N*-(1-undecyldodecyl)-*N*'-(6-hexyl)perylene-3,4,9,10-tetracarboxylic diimide]-2,7-dibromocarbazole was prepared according to a modified procedure by Blouin *et al* [19]. A mixture of *N*-(1-Undecyldodecyl)-*N*'-(6-hexyl-*p*-toluenesulfonate)perylene-3,4,9,10-tetracarboxylic diimide (1.02 g, 1.054 mmol) in DMSO (22 ml) and THF (18.5 ml) was added dropwise to a mixture of 2,7-dibromo-3,6-dimethyl-9*H*-carbazole (0.5629 g, 1.559 mmol) and freshly ground KOH (0.222 g, 3.956 mmol) in DMSO (11 ml). The reaction mixture was stirred for 36 h before THF was removed under high vacuum. Et₂O (500 ml) and H₂O (1 L) were added. To improve the phase separation NaCl was added also to the mixture. Then the mixture was extracted with Et₂O (5 x 500 ml). The collected organic layer was concentrated and the crude product was purified via column chromatography on silica gel, eluting with 99:1 chloroform/AcOH to obtain dark red solid (0.540 g, 44% yield). The product gave a single spot on TLC (99:1 CHCl₃/AcOH) ($R_f = 0.36$). ¹H NMR (CDCl₃) δ_H /ppm: 8.541 (m, 8H); 7.601 (d, 2H, $J = 8.48$); 7.495 (d, 2H, $J = 5.68$); 5.198 (m, 1H); 4.131 (t, 4H, $J = 7.38$ Hz); 2.281 (m, 2H); 1.876 – 1.641 (m, 6H); 1.488 (m, 4H); 1.2625 (m, 36H); 0.847 (t, 6H, $J = 6.28$ Hz). ¹³C-NMR (CDCl₃) δ_C /ppm: 162.38, 161.31, 161.09, 151.99, 150.09, 135.61, 132.40, 131.95, 129.61, 129.10, 128.85, 127.69, 127.30, 127.03, 125.76, 124.10, 124.02, 121.92, 121.19, 120.86, 120.80, 119.40, 119.37, 119.34, 119.30, 111.01, 105.90, 105.71, 104.91, 104.72, 68.37, 52.70, 41.54, 38.10, 29.76, 28.79, 27.47, 27.43, 27.19, 26.48, 25.58, 24.87, 24.66, 24.52, 20.52, 11.96. FT-IR (ATR): (cm⁻¹): 2922.2, 2851.6, 1693.6, 1650.7, 1594.0, 1467.5, 1440.1, 1404.4, 1338.4, 1247.2, 1159.6, 1124.4, 1081.7, 1040.0, 972.3, 852.2, 809.7, 792.9, 745.9, 618.1. Elemental Analysis (%) Calculated for C₆₅H₇₁Br₂F₂N₃O₄: C, 67.53%; H, 6.19%; N, 3.63%; Br, 13.82%. Found: C, 67.09%; H, 6.15%; N, 3.62%; Br, 13.93%. MALDI-TOF MS (monoisotopic mass = 1156.08); $m/z = 1155 [M + H^+]$.

1,4-Dibromo-2-fluoro-5-nitrobenzene (7)

1,4-Dibromo-2-fluoro-5-nitrobenzene was prepared according to the procedure by Chen *et al* [20]. 1,4-dibromo-2-fluorobenzene (100 g, 394 mmol) was dissolved in a 2:2:1 mixture of DCM (300 ml)/trifluoroacetic acid (300 ml)/trifluoroacetic anhydride (150 ml). The solution was cooled using an ice bath to 0 °C and then ammonium nitrate (38.8 g, 484 mmol) was added slowly with stirring. The mixture was allowed to warm to room temperature and left stirring overnight. Then the reaction mixture was poured onto ice (600 g) and the product was extracted with DCM (3 x 200 ml). The organic phase was dried over MgSO₄ and solvent removed in vacuo to give the crude product as a yellow solid. Which was then recrystallised from ethanol and yellow crystals were obtained and dried in vacuo to give 1,4-dibromo-2-fluoro-5-nitrobenzene (102.7 g, 87.24 % yield). The product gave a single spot on TLC ($R_f = 0.73$) in DCM/Hexane 1:1, m.p. 59.1- 62.7 °C. ¹H NMR (CDCl₃) δ_H /ppm: 8.205 (d, $J = 6.36$ Hz); 7.558 (d, $J = 7.36$ Hz). ¹³C NMR (CDCl₃) δ_C /ppm: 108.76 (d, $J_{C-F} = 23.77$ Hz); 114.91; 115.00; 122.74 (d, $J_{C-F} = 26.07$ Hz); 130.92; 161.89 (d, $J_{C-F} = 259.17$ Hz). FT-IR (ATR): (cm⁻¹): 3091.2; 3021.4; 2033.5; 1760.5; 1585.8; 1567.3; 1526.0; 1463.1; 1345.4; 1283.4; 1249.9; 1223.8; 1131.3; 1066.9; 933.3; 891.7; 869.1; 829.8; 752.3; 695.3; 643.9; 623.6. Mass (EI);

(m/z): 297, 299, 300 (M^{•+}); (calculated for C₆H₂N₂OBr₂F₂: 298.89). Elemental Analysis (%) calculated for C₆H₂N₂OBr₂F₂: C, 24.11; H, 0.67; N, 4.96; Br, 53.47. Found: C, 24.15; H, 0.59; N, 4.56; Br, 53.65.

4,4-Dibromo-5,5-difluoro-2,2-dinitro-biphenyl (8)

4,4-Dibromo-5,5-difluoro-2,2-dinitro-biphenyl was prepared according to the procedure by Yamato *et al* [21]. To 1,4-dibromo-2-fluoro-5-nitrobenzene (**7**) (50.89 g, 170.2 mmol) in dry DMF (250 ml) was added Cu Powder (14.42 g, 226.9 mmol) and the mixture was refluxed for 3 hours. The reaction mixture was cooled to ambient temperature and toluene was added (300 ml) and the mixture stirred for a further 1 hour. The un-reacted Cu powder was filtered off and the filtrate washed with a saturated NaCl solution. The organic layer was dried over MgSO₄ and the solvent removed *in vacuo* to give the crude product. The product was then recrystallized from ethanol and yellow crystals were obtained and dried *in vacuo* to give 4,4-dibromo-5,5-difluoro-2,2-dinitro-biphenyl (**8**) (26.5 g, 71.08 % yield). The product gave a single spot on TLC (R_f = 0.79) 8:2 (40-60 petroleum ether/ethyl acetate); m.p. 116.5-117.5 °C. Mass (EI); (m/z): 436, 438, 440 (M^{•+}). ¹H NMR (CDCl₃) δ_H/ppm: 8.54 (d, 2H, *J* = 5.96 Hz); 7.09 (d, 2H *J* = 7.85 Hz). ¹³C NMR (CDCl₃) δ_C/ppm: 110.31 (d, *J*_{C-F} = 26.84 Hz); 118.35 (d, 2C, *J*_{C-F} = 33.74 Hz); 131.11; 134.13; 142.80; 161.82 (d, *J*_{C-F} = 281.4 Hz). ATR cm⁻¹: 3104.2; 3071.4; 2106.0; 1609.7; 1564.8; 1520.9; 1489.8; 1463.7; 1403.9; 1335.6; 1288.5; 1227.4; 1184.1; 1113.9; 1065.6; 994.2; 902.5; 876.9; 846; 821.9; 760.2. Elemental Analysis (%) calculated for C₁₂H₄N₂O₄ F₂Br₂: C, 32.91; H, 0.92; N, 6.40; Br, 36.49. Found: C, 33.12; H, 0.83; N, 6.33; Br, 36.40.

4,4-Dibromo-5,5-difluoro-biphenyl-2,2-diamine (9)

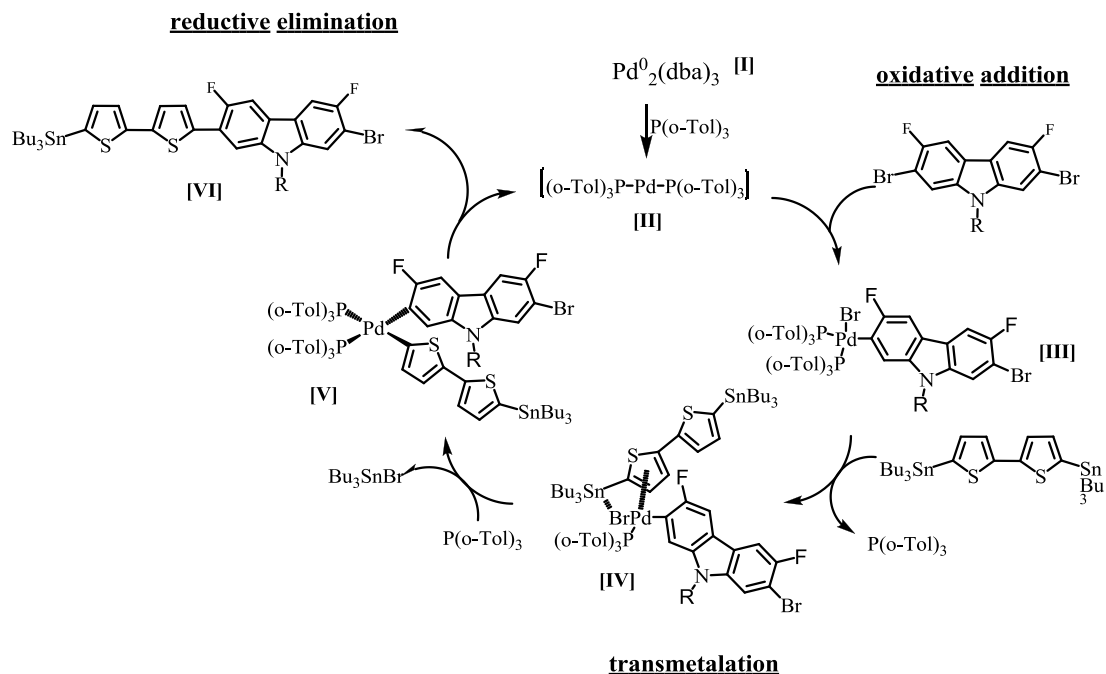
4,4-Dibromo-5,5-difluoro-biphenyl-2,2-diamine was prepared according to a modified procedure by Yamato *et al* [21]. 4,4-Dibromo-5,5-difluoro-2,2-dinitro-biphenyl (**8**) (11.60 g, 26.5 mmol) was dissolved in a solution of ethanol (160 ml) and HCl (45 ml, 32 % wt), tin powder (12.45 g, 104.8 mmol) was added. The reaction was taken to reflux for 90 mins and then cooled to room temperature and a further portion of tin powder (12.45 g, 104.8 mmol) was added and reflux for 1 hour. The reaction was again cooled to room temperature and the un-reacted tin powder was filtered off. The filtrate was poured onto ice and a 10 wt % solution of NaOH (1000 ml). The filtrate was then extracted with diethyl ether (4 x 250 ml) and the resulting fine white suspension was filtered using Celite® filter gel and washed with diethyl ether. The organic layer was washed with distilled H₂O (3 x 200 ml), dried over MgSO₄ and the solvent removed *in vacuo* to give a brown solid. The product was then recrystallised from ethanol to obtain pale brown crystals and dried *in vacuo* to give 4,4-dibromo-5,5-difluoro-biphenyl-2,2-diamine (**9**). (9.44 g, 94.30 % yield). The product gave a single spot on TLC (R_f = 0.41) 8:2 40-60 petroleum ether/ ethyl acetate; m.p. 163-168 °C. Mass (EI); (m/z): 376, 378, 380 (M^{•+}). ¹H NMR (CDCl₃) δ_H/ppm: 3.69 (b, 4H); 6.89 (d, 2H, *J* = 8.8 Hz); 6.98 (d, 2H, *J* = 6.1 Hz). ¹³C NMR (CDCl₃) δ_C/ppm: 109.30 (d, *J*_{C-F} = 21.47 Hz); 118.08 (d, *J*_{C-F} = 23 Hz); 119.75; 122.82; 141.01; 153.57 (d, *J*_{C-F} = 239.23 Hz). ATR cm⁻¹: 4309.7; 3191.5; 2358.3; 2193.9; 1622.1; 1483.6; 1406.0; 1297.8; 1274.4; 1241.9; 1196.3; 1163.8; 1056.4; 992.3; 889.3; 867.5; 815.0; 757.2; 702. Elemental analysis calculated for C₁₂H₈N₂Br₂: C, 38.13; H, 2.13; N, 7.41; Br, 42.28. Found: C, 38.72; H, 2.04; N, 7.47; Br, 42.34.

2,7-Dibromo-3,6-difluoro-9H-carbazole (10)

2,7-Dibromo-3,6-difluoro-9H-carbazole was prepared according to the procedure by Sonntag *et al* [22]. To 4,4-dibromo-5,5-difluoro-biphenyl-2,2-diamine (**9**) (4 g, 10.58 mmol) was added concentrated phosphoric acid (85%) (88 ml) and the mixture heated at 180 °C for 24 hours. The crude product was filtered and washed with water. The crude product was then solubilised in toluene and the solution filtered through a silica gel plug and dried over MgSO₄. The solvent was removed in vacuo to give ivory powder. The crude product was recrystallised from toluene/hexane (10:1) to give the product as an ivory powder (2.77 g, 72.51 % yield). The product gave a single spot on TLC (R_f = 0.43) 8:2 40-60 petroleum ether/ethyl acetate, m.p. 255 – 260.5 °C. Mass (EI); (m/z): 359, 361, 362 (M⁺). ¹H NMR (Acetone-d₆) δ_H/ppm: 7.86 (d, 2H, J = 5.62 Hz); 8.10 (d, 2H, J = 9.54 Hz); 10.69 (br, 1H). ¹³C NMR (Acetone-d₆) δ_C/ppm: 107.92 (d, J_{C-F} = 23.77 Hz); 108.17; 116.41; 123.2; 138.79; 155.13 (d, J_{C-F} = 236.17 Hz). ATR cm⁻¹: 3451.2; 3042.2; 1944.2; 1704.7; 1615.8; 1572.1; 1477.5; 1442.9; 1350.2; 1279.6; 1257; 1205.9; 1177.3; 1151.5; 1039.4; 991.2; 909.5; 857.6; 836.6; 788.1; 719.3; 676.0; 626.2; Elemental Analysis (%) calculated for C₁₂H₅NF₂Br₂: C, 39.93; H, 1.40; N, 3.88; Br, 44.27. Found: C, 39.24; H, 1.07; N, 3.96; Br, 44.44.

Synthesis of the polymer (PFCBT-PDI)

PFCBT-PDI was prepared according to a modified procedure by Wakim *et al* [23]. A solution of (**6**) (0.4024 g, 0.348 mmol), 5,5'-bis(tri-*n*-butylstannyl)-2,2'-bithiophene (0.2590 g, 0.3479 mmol), tri-*o*-tolylphosphine (0.0084 g, 0.0277 mmol) and tris(dibenzylideneacetone)dipalladium(0) (0.0063 g, 0.0068 mmol) in toluene (7 ml) was stirred for 22 h at 100°C. Then the solution was cooled down to room temperature followed by the addition of 2-(tributylstannyl)-thiophene (0.1947 g, 0.5219 mmol) and (10 ml) of toluene. The solution was stirred overnight at 100°C. Then another (10 ml) of toluene was added to the solution before it was heated to 100° C and then precipitated in (500 ml) of methanol. The obtained polymer was filtered and then was subjected to a soxhlet extraction with methanol (24 h), acetone (24 h), toluene (48 h) and CHCl₃ (48 h). The insoluble polymer left in the thimble was put into CHCl₃ and stirred to reflux for 8 hours before the solution was concentrated to approx. 10 ml and the polymer precipitated in methanol (500 mL) to provide a first fraction of the polymer after filtration (0.012 g, 2.89% yield). The insoluble polymer left in the thimble was subject again to a soxhlet extraction with Chlorobenzene (48 h) before the solution was concentrated to approx. 10 ml and the polymer precipitated in methanol (500 mL) to provide a second fraction of the polymer after filtration (0.134 g, 32.36% Yield). ¹H NMR (CDCl₃) δ_H/ ppm: 8.377 (m, 8H); 7.612 (bs, 2H); 7.401 (bs, 2H); 7.178 (bs, 2H); 7.039 (bs, 2H); 5.106 (m, 1H); 4.172 (b, 4H); 2.300 (b, 2H); 1.885 – 1.712 (m, 6H); 1.309 (m, 4H); 1.187 (m, 36H); 0.847 (t, 6H, J = 6.28 Hz). Elemental Analysis (%) for second fraction of polymer: Calculated for C₇₅H₈₁F₂N₃O₄S₂: C, 75.66%; H, 6.86%; N, 3.53%; S, 5.39%. Found: C, 49.15%; H, 7.39%; N, 1.29%; S, 3.27%. GPC (CHCl₃) – first fraction of polymer: M_n = 4500; M_w = 9300; PD = 2.1. GPC (CHCl₃) – second fraction of polymer: M_n = 62000; M_w = 96000; PD = 1.5



Scheme 2. The proposed mechanism of the Stille coupling by Santos *et al.*

In the first step $\text{Pd}_2(\text{dba})_3$ reacts with two $\text{P}(\text{o-Tol})_3$ to give the catalytically active complex $[\text{Pd}(\text{P}(\text{o-Tol})_3)_2]$ **[II]**. The second step is an oxidative addition of the carbazole-based co-monomer (**10**) (the electrophile) to the Pd^0 to give the cis-product at first, which then isomerizes to form the trans-complex **[III]**. The third step is transmetalation reaction, at first, one of the phosphine ligand ($\text{P}(\text{o-Tol})_3$) is substituted by the organostannane compound (**29**) to produce a cyclic intermediate **[IV]**, involving an electrophilic attack of the Pd and a nucleophilic attack of the bromine ligand, which then reacts to **[V]**. The last step is reductive elimination, where the target product is eliminated and the catalytic cycle starts again.

In order to remove palladium impurities, oligomers and unreacted monomers, the crude polymer was purified by using several methods. After the polymerization the reaction mixture in toluene was precipitated in methanol to remove end-capping reagents, organic palladium species and unreacted co-monomers. Due to the insolubility of the formed polymer in the solvent at room temperature, the solution was heated before precipitation.

The obtained crude polymer was then collected through filtration on micropore membranes then transferred to a fiber glass thimble and cleaned with different solvents using a Soxhlet apparatus. The first solvent was methanol to remove the palladium residues from the copolymer and also to hydrolyze the residual tributyl-tin end groups, followed by acetone and toluene, to clean off the low molecular weight oligomers. Then the purified polymer was extracted with chloroform (CHCl_3) for 48 hours and the solutions precipitated again in methanol to obtain the first fraction of the polymer. However, not all the polymer inside the thimble dissolved, therefore chlorobenzene ($\text{C}_6\text{H}_5\text{Cl}$) was used to extract the remaining insoluble polymer and obtain the second fraction of the polymer.

GPC analysis of the polymer which was extracted by chloroform (CHCl_3) gave the $M_w = 9300$ and $M_n = 4500$ with a polydispersity of 2.1 and the degree of polymerization as 4, therefore there are an

average approximately 4 carbazole units per polymer chain. While the GPC analysis of the polymer which was extracted by chlorobenzene (C_6H_5Cl) gave the $M_w = 96000$ and $M_n = 63000$ with a polydispersity of 1.5 and the degree of polymerisation as 54, therefore there are average approximately 54 carbazole units per polymer chain.

The polymerization was left for 48 hours; therefore, approx. 92 % of the polymer was insoluble in $CHCl_3$, so the majority of the polymer was extracted by chlorobenzene. This is because of the high molecular weight of the polymer. The pendent perylene units are thought to be able to form stacks, which may have an effect on the solubility of the polymer.

1H -NMR spectra of the polymer in $CDCl_3$ are not clear because the obtained signals are very broad. Especially in the aromatic region (6 – 9 ppm) there is only one broad peak. Ahrens *et al.* [26] observed this phenomenon for donor-acceptor copolymers which contain several PDI molecules and such observation were linked to the PDIs aggregation. In the case of polymer (**P1**), the aggregation between PDI moieties of the same polymer backbone is more likely to cause this broad peak, rather than from different backbones. However, Catellani *et al.* [27] reported that it is possible to break this aggregation by carrying out the NMR analysis at high temperature.

Figure 2 and Figure 3 show the 1H -NMR of solution of polymer (**P1**) in $C_2D_2Cl_4$ at 100 °C and room temperature respectively. A sharpening of the peaks in the aromatic region appeared, indicating that aggregation of PDI moieties is reduced to a certain level at higher temperatures. The PDI units can be identified from signals of their eight protons on their aromatic rings and show up as a multi peaks between 8.0 ppm and 8.6 ppm. Signals from the carbazole protons and dithienyl protons are observed between 7.00 and 7.70 ppm. The other peaks correspond to the protons of the hexyl-linkage between the PDI molecule and the polymer backbone or the tricosanyl chains, and they are in agreement with the NMR data which are observed for compound (**10**).

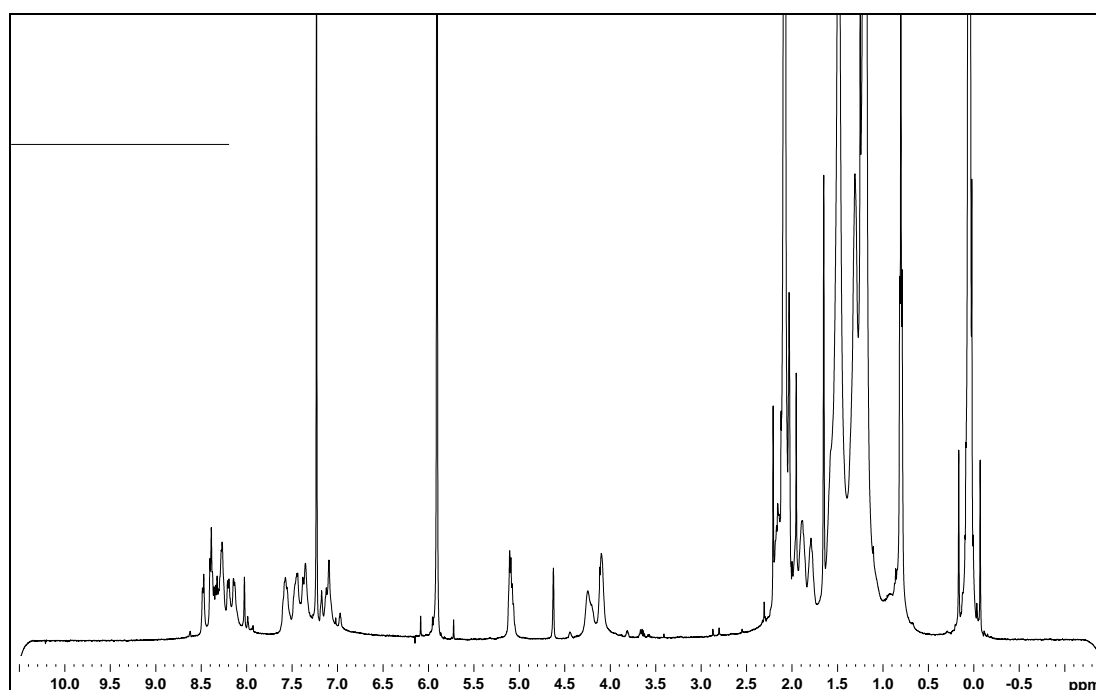


Figure 2. 1H -NMR spectra of the polymer in $C_2D_2Cl_4$ at 100 °C

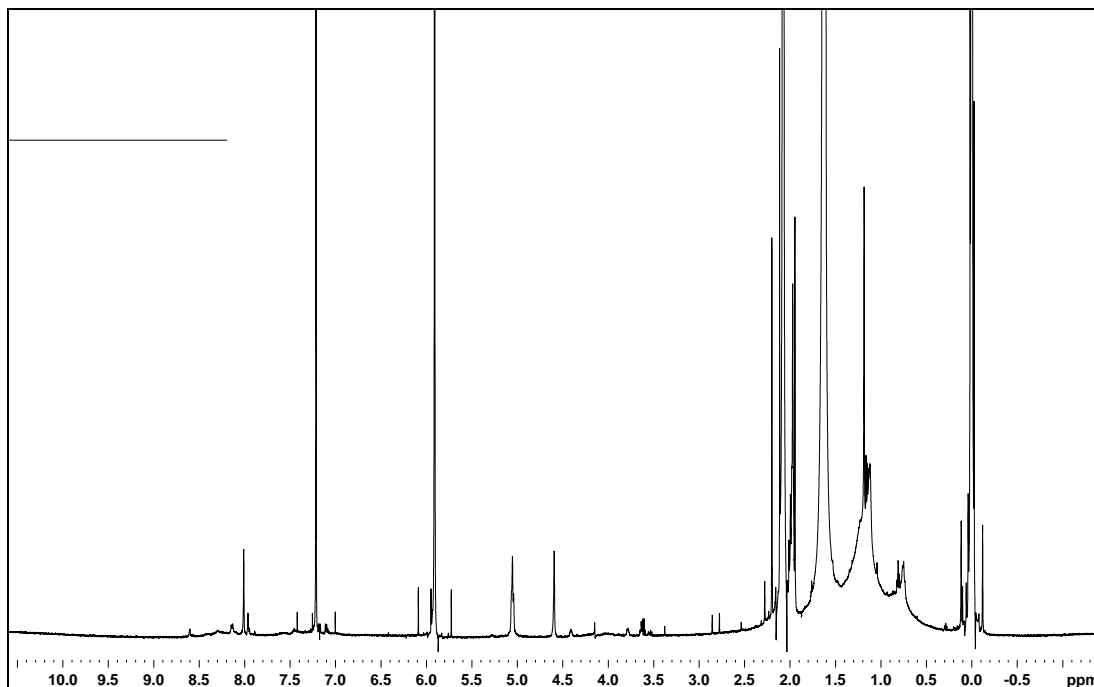


Figure 3. $^1\text{H-NMR}$ spectra for the same sample of the polymer in $\text{C}_2\text{D}_2\text{Cl}_4$ at room temperature

3.2 Thermo-gravimetric Analysis (TGA)

Figure 4 shows the TGA curves of the thermal degradation of the polymer, the onset of the degradation occurs at $386\text{ }^\circ\text{C}$, the onset of second degradation is $460\text{ }^\circ\text{C}$ with a weight loss of 72.3% . The percentage of residual weight (31.4%) is consistent with percentage weight of PDI units and polymer backbone. The TGA analysis confirms that the polymer has a high thermal stability up to $380\text{ }^\circ\text{C}$.

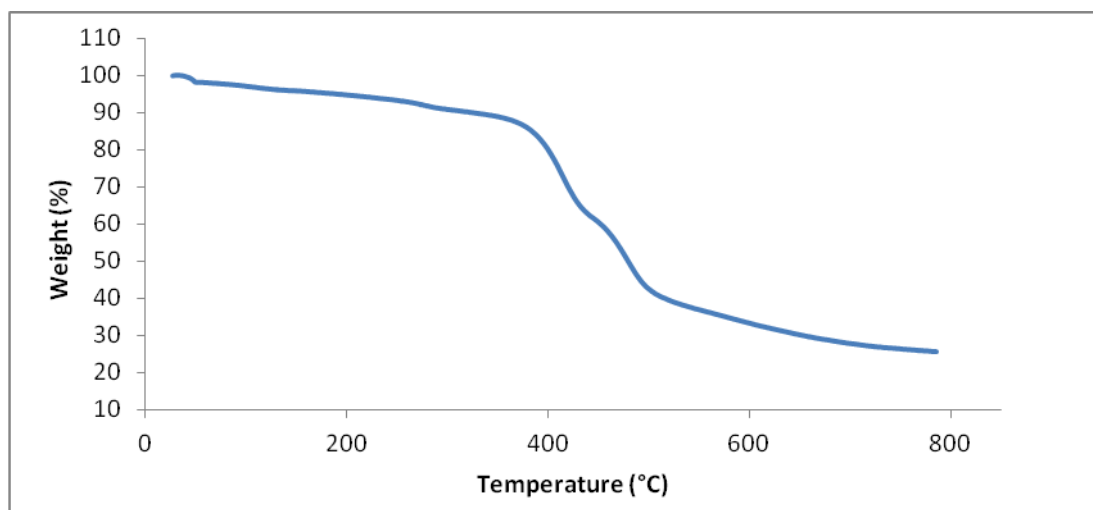


Figure 4. The TGA thermogram of PFCBT-PDI

Differential Scanning Calorimetry (DSC) analysis

The DSC thermogram for the polymer (second fraction) does not display any clear glass transition (T_g) in the first heating scan or the second heating and cooling scan. The small peak at -41 °C appeared only in the first heating scan, indicating that it represented the melting of crystals which formed by solvent recrystallization [17]. The analogous polymer PCB-PDI also did not show a clear glass transition (T_g) in the first heating scan or the second heating and cooling scan.

3.3 UV-Visible absorption spectroscopy analysis

Figure 5 shows the absorption spectra of the polymer in chloroform, toluene and THF solutions and in solid state as thin films. The results of these studies are summarized in Table 1.

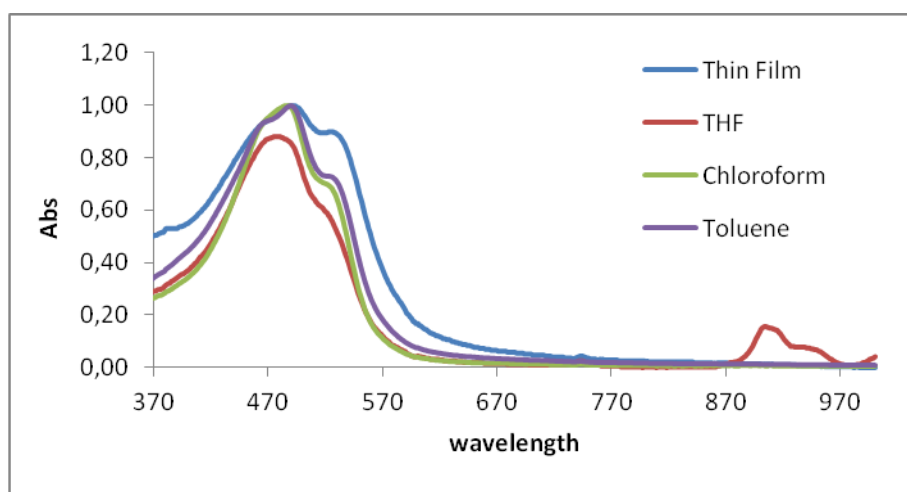


Figure 5. Normalised absorption spectra of the polymer in different solvent and thin film

The absorption spectra display main broad absorption bands with small shoulders at λ_{\max} 488 nm and 523 nm in chloroform solution, at 481 nm and 526 nm in THF solution, at 491 nm and 532 nm in toluene solution and at 494 nm and 537 nm in the solid state. The optical band gap is 2.10 eV, from the onset of the absorption band in the solid state.

Table 1. UV-vis data of the polymer in different solvent and thin film

	$\lambda_{\max 1} / \text{nm}$	$\lambda_{\max 2} / \text{nm}$
Chloroform solution	488	523
THF solution	481	526
Toluene solution	491	532
Thin film	494	537

The strong absorption bands at (481-494 nm) are thought to correspond to the carbazole-bithiophene backbone of the polymer while the shoulder bands at (523-537 nm) come from the absorption of the PDI units on the polymer. The slight difference between absorption maxima in the different solvents arises from the solvatochromism phenomenon [28]. The slight shift of λ_{\max} between the solutions and the thin film is expected, as the structure of the polymer is more planar and the freedom of movement is limited in the solid state, therefore the overlap of p_z -orbitals is better and the electronic delocalization is higher.

The absorption spectra in the polar solvent THF display another absorption band ($\lambda_{\max 3} = 916$) with shoulder ($\lambda_{\max 4} = 949$) which could arise from an intramolecular electron transfer between PDI-units and polymer backbone. It is worth noting that such bands were not observed for an equivalent polymer (PCB-PDI) reported in the literature by the Iraqi's group [29], which had methyl substituents instead of fluoro substituents on the carbazole repeat units.

Comparison of this result to that of the equivalent polymer (PCB-PDI) indicates a higher band gap of 2.19 eV for the polymer with methyl substituents on the carbazole repeat units. This difference is because of the size of methyl groups which is larger than that of fluoro groups, resulting in higher degree of twisting between the bithiophene and the carbazole repeat units along the polymer backbone and leading to a decrease in the electronic conjugation and a slight increase in the band gap.

Comparison of UV-Vis results of PFCBT-PDI to those of PDI units and another equivalent polymer (PFCBT) which does not have PDI units and was prepared by Iraqi's group (Figure 6) shows that the λ_{\max} value of PFCBT-PDI (491 nm) comes between the λ_{\max} of PDI units (497 nm) and the λ_{\max} of PFCBT (482 nm), and the absorption spectrum of PFCBT-PDI in thin film consists of an approximate superposition of the absorption spectra of PDI units and PFCBT. The absorption bands at 491 nm and 527 nm could be assigned as originating from PDI substituents on PFCBT-PDI while the absorption bands at 467 nm and 491 nm arise from the absorption of the carbazole-bithiophene backbone of the polymer (Figure 7).

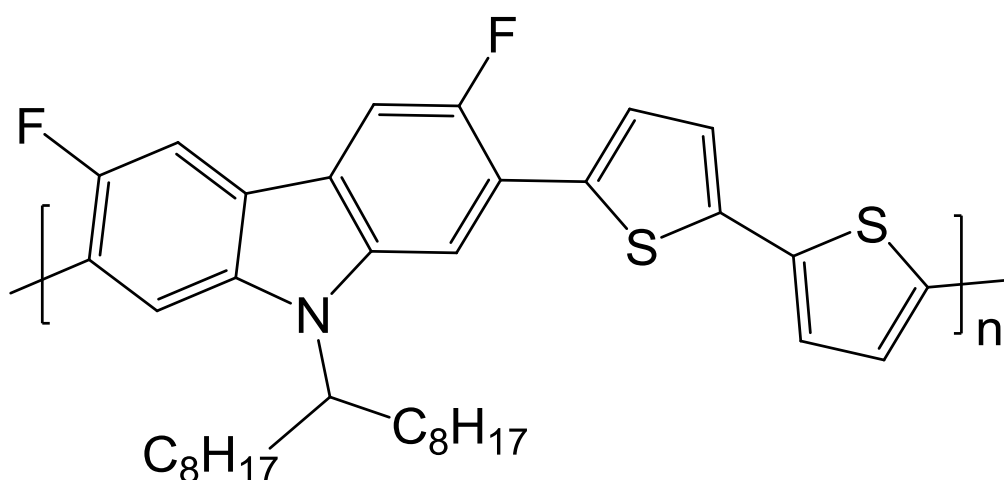


Figure 6. The equivalent polymer PFCBT

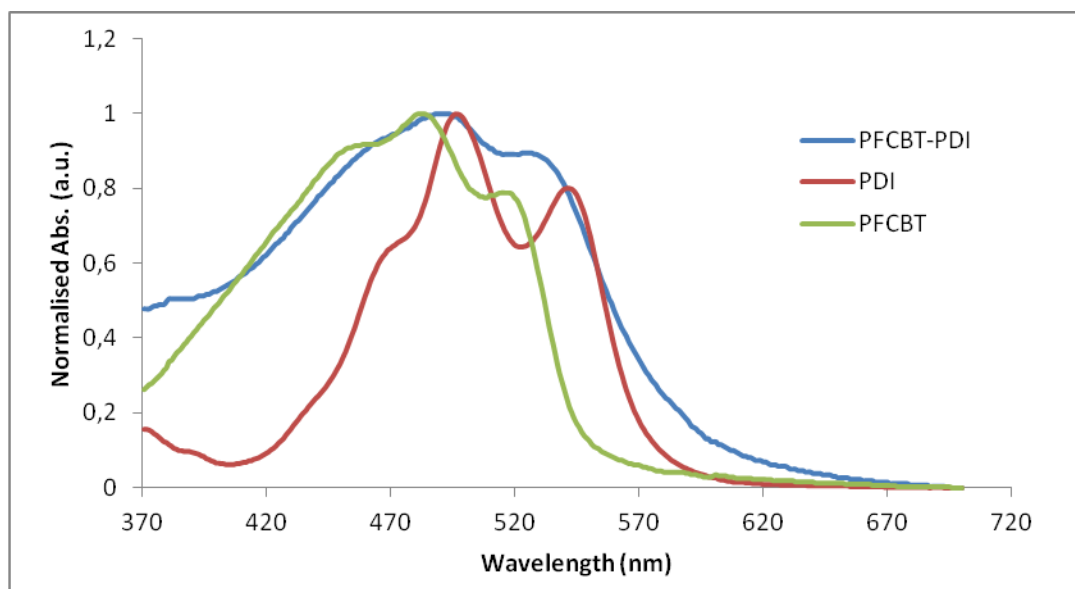


Figure 7. Normalised UV-Vis spectra of PFCBT-PDI, PFCBT and PDI units as thin film

3.4 Photoluminescence spectroscopy analysis

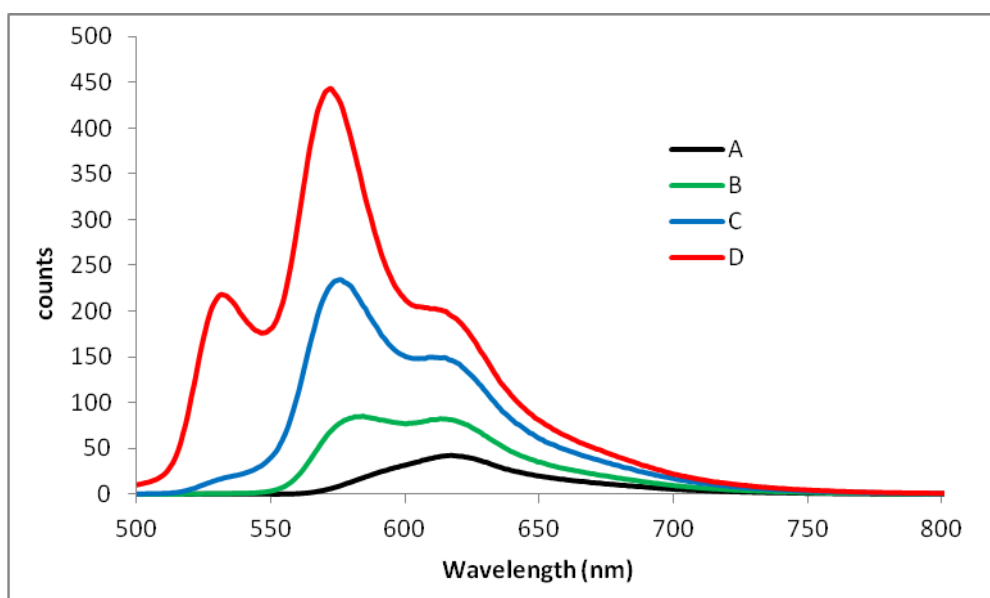


Figure 8. Fluorescence spectra of (P1) in solutions of THF at different concentrations

This analysis shows the quenching effect induced by the PDI moieties in the polymer and also the role of PDI units in the exciton dissociation, the emission intensity displays the degree of the quenching by PDI units. Figure 8 shows the emission spectra of PFCBT-PDI in solutions of THF at concentrations $A \cong 1 \times 10^{-6}$ M, $B \cong 5 \times 10^{-7}$ M, $C \cong 2.5 \times 10^{-7}$ M and $D \cong 1.25 \times 10^{-7}$ M. At concentration D the photoluminescence spectra show three main bands centered at 531 nm, 571 nm and 614 nm, when the excitation wavelength was chosen as 485 nm. The emission intensity increases with decreasing of the solution concentration. This could be due to a decrease of intermolecular

interactions between polymer chains. At high concentration the emission of the polymer was quenched. It is however difficult to postulate the exact nature of intermolecular interactions which lead to this result i.e. whether it is due to interaction of PDI units from different polymer chains or that from PDI units of one polymer chain with the backbone of a different polymer chains.

Comparison of photoluminescence results of PFCBT-PDI in solution at the highest concentration A and the lowest concentration D to those of the PDI units in Figure 9 shows that the emission spectra of PDI units disappear at high concentration A, while in low concentration D they can be observed. Moreover, the emission spectra of PFCBT-PDI at high concentration show incomplete quenching of fluorescence comparing to the equivalent polymer (PCB-PDI) which exhibits complete quenching [29], this difference *is perhaps due to* the presence of the fluorine substituents on the carbazole that may prevent complete electron transfer from the polymer chain to the PDI units.

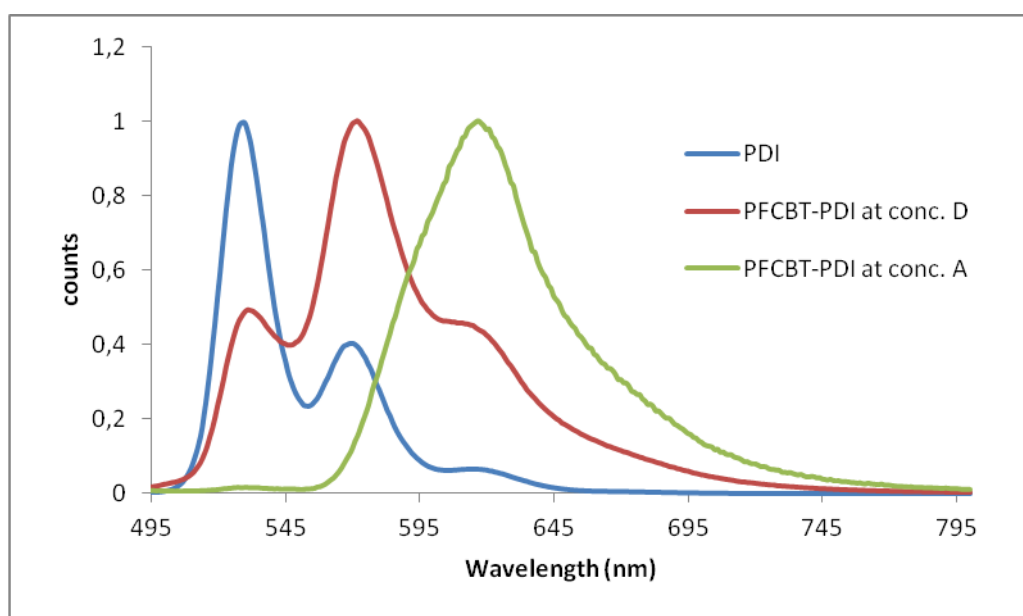


Figure 9. Normalised fluorescence spectra of PFCBT-PDI in solution at the highest concentration A and the lowest concentration D, and PDI units

3.5 Cyclic Voltammetry (CV) analysis

Cyclic voltammetry (CV) studies were performed on drop-cast polymer films in acetonitrile with tetrabutylammonium perchlorate as the electrolyte. The electron affinities (E_A) and the ionization potentials (I_P) were calculated from the onset reduction and oxidation. Then the electrochemical band gap can be calculated from the difference between the electron affinity (E_A) (or LUMO) and the ionization potentials (I_P) (or HOMO). The cyclic voltammogram of the polymer is shown in Figure 10.

The polymer backbone exhibits an oxidation wave at $E_{pa} = +0.75$ V and a reduction wave at $E_{pa} = -2.35$ V, and their associated reduction and oxidation at $E_{pc} = +0.64$ V and $E_{pc} = -2.13$ V respectively. The PDI unit can be obviously identified by the reduction wave at $E_{pa} = -1.37$ V and the associated oxidation wave at $E_{pc} = -0.98$ V.

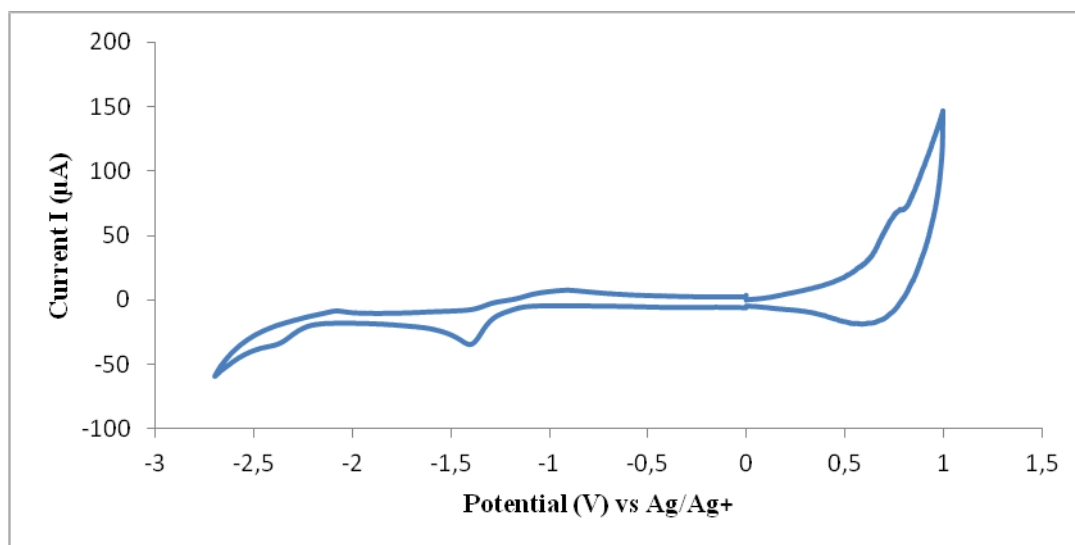


Figure 10. Cyclic voltammogram spectra of the polymer PFCBT-PDI

From the onset of oxidation (+0.58 V) and the onset of reduction (-2.22 V), the polymer HOMO or ionization potential, $I_p = -5.29$ eV and the LUMO or electron affinity, $E_A = -2.49$ eV for the polymer backbone (on the basis that ferrocene/ferrocenium has an I_p of 4.8 eV below the vacuum level and the oxidation occurs at 0.082 V relative to Ag/Ag^+), therefore the electrochemical band gap of the polymer is 2.8 eV. The E_A or LUMO of the PDI moiety is -3.47 eV, calculated from the onset of reduction at -1.24 V, therefore the position of the LUMO (-3.47 eV) of the PDI unit would allow a high open circuit voltage (1.82 eV) in the solar cell applications (Figure 11). This slight difference between the optical band gap (2.10 eV) and the electrochemical band gap (2.8 eV) is not uncommon in literatures that the electrochemical band gap in many studies is higher than the optical band gap [30].

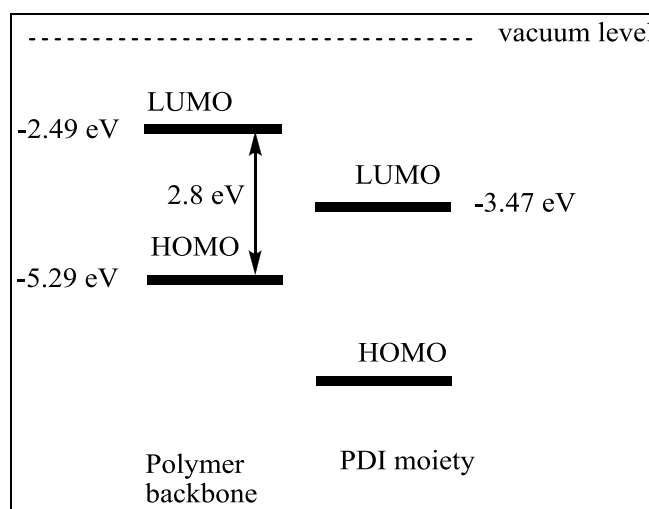


Figure 11. Energy level alignment for PFCBT-PDI

The comparison of this result to that of the equivalent polymer (PCB-PDI) prepared by Iraqi's group [29], which have methyl groups at the 3- and 6-positions on the carbazole ring, displays a higher electrochemical band gap of 2.9 eV. This difference is, again, because of the size of methyl groups is larger than fluoro groups, resulting in higher degree of twisting between the bithiophene and the

carbazole repeat units along the polymer backbone and leading to a decrease in the electronic conjugation and a slight increase in the band gap. Moreover, there is a slight difference between LUMO levels of PDI units in PFCBT-PDI (-3.47 eV) and the PDI units in the equivalent polymer (PCB-PDI) (-3.74 eV).

Table 2. Electrochemical data of PFCBT-PDI, PDI units and the analogous polymer PCB-PDI

Polymers	[O] ₁ (V)	[R] ₁ (V)	I _p (eV)	E _A (eV)	E _g (eV)
	E _{1/2} (V)	E _{1/2} (V)			
PFCBT-PDI	0.97	-2.24	-5.29	-2.49	2.80
PDI	-	-1.18	-	-3.47	-
PCB-PDI	0.58	-2.39	-5.38	-2.48	2.90
PDI	-	-1.22	-	-3.74	-

4. CONCLUSION

A novel “double-cable” polymer PFCBT-PDI was successfully synthesized *via* Stille cross-coupling polymerization, the photophysical and electrochemical properties show that the optical and electrochemical band gaps of PFCBT-PDI are smaller than those of an analogous polymer PCB-PDI which has methyl substituents on carbazole repeat units since the fluoro groups on PFCBT-PDI are smaller than methyl groups, leading to a decrease in steric hindrance which enables more extended electronic conjugation on the new polymer. The electrostatic interaction between fluorine substituents on carbazole repeat units and the hydrogens at the 4-position of neighboring thiophene rings do also support the planarity and electronic conjugation along the polymer chains. However, photoluminescence measurements on PFCBT-PDI in solution show incomplete quenching of fluorescence as compared to the equivalent polymer PCB-PDI which exhibits complete fluorescence quenching. This difference is perhaps due to the presence of the fluorine substituents on the carbazole repeat units that may prevent complete electron transfer from the polymer chain to the pendent PDI units.

ACKNOWLEDGEMENTS

This research was supported by King Saud University, deanship of Scientific Research, College of Science Research center.

References

1. H. Spanggaard and F. C. Krebs, *Solar Energy Materials and Solar Cells*, 83 (2004) 125.

2. S. Günes, H. Neugebauer and N. S. Sariciftci, *Chem. Rev*, 107 (2007) 1324.
3. C. J. Brabec, N. S. Sariciftci and J. C. Hummel, *Advanced Functional Materials*, 11 (2001) 15.
4. C. J. Brabec and S. N. Sariciftci, *Monatshefte für Chemie/Chemical Monthly*, 132 (2001) 421.
5. A. Cravino and N. S. Sariciftci, *Journal of Materials Chemistry*, 12 (2002) 1931.
6. A. Cravino, G. Zerza, M. Maggini, S. Bucella, M. Svensson, M. R. Andersson, H. Neugebauer, C. J. Brabec and N. S. Sariciftci, *Monatshefte für Chemie/Chemical Monthly*, 134 (2003) 519.
7. A. Cravino, G. Zerza, H. Neugebauer, S. Bucella, M. Maggini, E. Menna, G. Scorrano, M. Svensson, M. R. Andersson and N. S. Sariciftci, *Synthetic Metals*, 121 (2001) 1555.
8. S. Luzzati, M. Scharber, M. Catellani, N. O. Lupsac, F. Giacalone, J. L. Segura, N. Martín, H. Neugebauer and N. S. Sariciftci, *Synthetic Metals*, 139 (2003) 731.
9. Z. a. Tan, J. Hou, Y. He, E. Zhou, C. Yang and Y. Li, *Macromolecules*, 40 (2007) 1868.
10. L. Feng and Z. Chen, *Polymer*, 46 (2005) 3952.
11. R. Gómez, D. Veldman, R. I. Blanco, C. Seoane, J. L. Segura and R. A. J. Janssen, *Macromolecules*, 40 (2007) 2760.
12. K. Balakrishnan, A. Datar, T. Naddo, J. Huang, R. Oitker, M. Yen, J. Zhao and L. Zang, *J. Am. Chem. Soc.*, 128 (2006) 7390.
13. H. Langhals, H. Jaschke, H. Bastani Oskoui and M. Speckbacher, *European Journal of Organic Chemistry*, 2005 (2005) 4313.
14. Y. Che, A. Datar, K. Balakrishnan and L. Zang, *Journal of the American Chemical Society*, 129 (2007) 7234.
15. J. C. Antilla, A. Klapars and S. L. Buchwald, *J. Am. Chem. Soc.*, 124 (2002) 11684.
16. L. X. Chen, S. Xiao and L. Yu, *J. Phys. Chem. B*, 110 (2006) 11730.
17. B. Jancy and S. K. Asha, *The Journal of Physical Chemistry B*, 110 (2006) 20937.
18. Y. Yoshida, Y. Sakakura, N. Aso, S. Okada and Y. Tanabe, *Tetrahedron*, 55 (1999) 2183.
19. N. Blouin, A. Michaud and M. Leclerc, *Advanced Materials*, 19 (2007) 2295.
20. N. Choy, K. C. Russell, J. C. Alvarez and A. Fider, *Tetrahedron Letters*, 41 (2000) 1515.
21. T. Yamato, C. Hideshima, M. Tashiro, G. K. S. Prakash and G. A. Olah, *J. Org. Chem.*, 56 (1991) 6248.
22. M. Sonntag and P. Strohrriegl, *Chem. Mater*, 16 (2004) 4736.
23. S. Wakim, N. Blouin, E. Gingras, Y. Tao and M. Leclerc, *Macromolecular Rapid Communications*, 28 (2007) 1798.
24. J. K. Stille, *Angew. Chem., Int. Ed. Engl.*, 25 (1986) 508.
25. L. S. Santos, G. B. Rosso, R. A. Pilli and M. N. Eberlin, *J. Org. Chem.*, 72 (2007) 5809.
26. M. J. Ahrens, R. F. Kelley, Z. E. X. Dance and M. R. Wasielewski, *Physical Chemistry Chemical Physics*, 9 (2007) 1469.
27. M. Catellani, S. Luzzati, N. O. Lupsac, R. Mendichi, R. Consonni, A. Famulari, S. V. Meille, F. Giacalone, J. L. Segura and N. Martín, *Journal of Materials Chemistry*, 14 (2004) 67.
28. Y. Li, H. Zheng, Y. Li, S. Wang, Z. Wu, P. Liu, Z. Gao, H. Liu and D. Zhu, *The Journal of Organic Chemistry*, 72 (2007) 2878.
29. D. K. Mohamad, A. Fischereder, H. Yi, A. J. Cadby, D. G. Lidzey and A. Iraqi, *J. Mater. Chem.*, 21 (2010) 851.
30. S. Admassie, O. Inganäs, W. Mammo, E. Perzon and M. R. Andersson, *Synthetic Metals*, 156 (2006) 614.